Technical insights into fluorescence lifetime microscopy of mechanosensitive Flipper probes.

Chloé Roffay[1], Juan Manuel Garcia Arcos[1], Pierrik Chapuis[1], Javier López-Andarias[2,3], Adai Colom[4,5,6], Caterina Tomba[7], Ilaria Di Meglio[1], Stefan Matile[2,3], Aurélien Roux[1,5]*, Vincent Mercier[1,5]*

[1]Department of Biochemistry, University of Geneva, CH-1211 Geneva, Switzerland.
[2]School of Chemistry, University of Geneva, CH-1211 Geneva, Switzerland.
[3]National Center of Competence in Research in Chemical Biology, University of Geneva, CH-1211 Geneva, Switzerland.
[4] Biofisika Institute (CSIC, UPV/EHU), 48940 Leioa, Spain;
[5] Department of Biochemistry and Molecular Biology, Faculty of Science and Technology, Campus Universitario, University of the Basque Country (UPV/EHU), 48940 Leioa, Spain
[6] IKERBASQUE, Basque Foundation for Science, 48013 Bilbao, Spain
[7] Univ Lyon, CNRS, INSA Lyon, Ecole Centrale de Lyon, Université Claude Bernard Lyon 1, CPE Lyon, INL, UMR5270, Villeurbanne 69622, France

*correspondence to: aurelien.roux@unige.ch, vincent.mercier@unige.ch;

Abstract: Measuring forces within living cells remains a technical challenge. We developed hydrophobic mechanosensing fluorescent probes called Flippers, which fluorescence lifetime depends on lipid packing and can report membrane tension. We describe here technical optimization of the probe imaging, and diverse characterizations in various biological and in vitro systems. We propose to the cell biology community a guideline to measure biophysical parameters of cellular membranes by FLIM microscopy with Flipper probes.[i]

Introduction

Measuring physical forces in biological material is of increasing interest, but remains technically challenging[1]. The possibility of measuring such forces through microscopy imaging presents the advantages of being less intrusive than many mechanical methods, makes use of the universally available microscopy equipment in research labs. Many fluorescence tools have been developed in this regard, in particular Forster Resonance Energy Transfer (FRET) biosensors, in which the elongation of a linker between two FRET fluorophores under force reduces FRET efficiency. The FRET couple and the linker can be composed of fluorescent proteins connected by a peptide chain, all being easily expressed in cells using standard molecular biology techniques. This has been developed to measure forces at focal adhesions, and have been extended to measure force between membranes and actin[2], the cytoskeleton and the nucleoskeleton[3] or under shear stress[4]. However, these biosensors have several limitations,

namely that the force range is very small and thus require the use of several chimeric constructs with different linkers. Also, it requires the force sensor to be bound to proteins "handles" onto which the force is applied and finding the right combination of interacting domains that will not detach under force remains challenging.

Another strategy has been to design small chemicals whose fluorescence properties will change under force variation. For example, molecular rotors based on Fluorescence Lifetime Imaging Microscopy (FLIM) were designed to measure viscosity in membranes[5,6]. One of the challenges has been to expand the list of forces that can be measured, as some of the forces are exerted within materials, and not between materials. We have designed, synthesized and characterized small-molecules called FLIPPERS that can report changes of membrane lateral forces due to lipid packing variations through changes of their conformation and hence of their fluorescence properties[7]. The high sensitivity of Flippers allows them to report membrane tension variations by changes of the lifetime of their excited state or fluorescence lifetime[8], upon osmotic shocks[9,10] or to investigate lysosomal exocytosis[11]. Over the past 6 years, we designed various derivatives targeting different organelles[12] (plasma membrane, endoplasmic reticulum, mitochondria and lysosome/late endosome). We also developed probes with different biochemical and/or photochemical properties[6] (HaloFlipper, HaloPhotoFlipper, HydroFlipper). We identified fluorescence lifetime imaging (FLIM) as the best way to report the conformational changes of Flipper probes with lipid packing. However, measuring membrane tension using FLIM of Flippers remains technically challenging. This method paper aims at bringing technical and practical information to make the use of Flipper probes for membrane tension measurements more accessible.

I-Basics of Flipper probes

Four commercialized Flipper probes with identical mechano-chemistry principle target different membranes in cells: Flipper-TR for plasma membrane, ER Flipper-TR for endoplasmic reticulum, Lyso Flipper-TR for late endo/lysosomes and Mito Flipper-TR for mitochondria. The common chemical structure of Flipper probes (see Fig 1a) is composed of two dithienothiophenes (DTT) fluorescent groups that can rotate around the carbon bond that links them together. Methyl groups have been added at specific places to ensure that the two DTT groups are twisted out of co-planarity in the ground state, but can still be planarized under application of orthogonal forces. Thus, Flippers have been designed as molecular sensors for compressive forces.

FIGURE 1

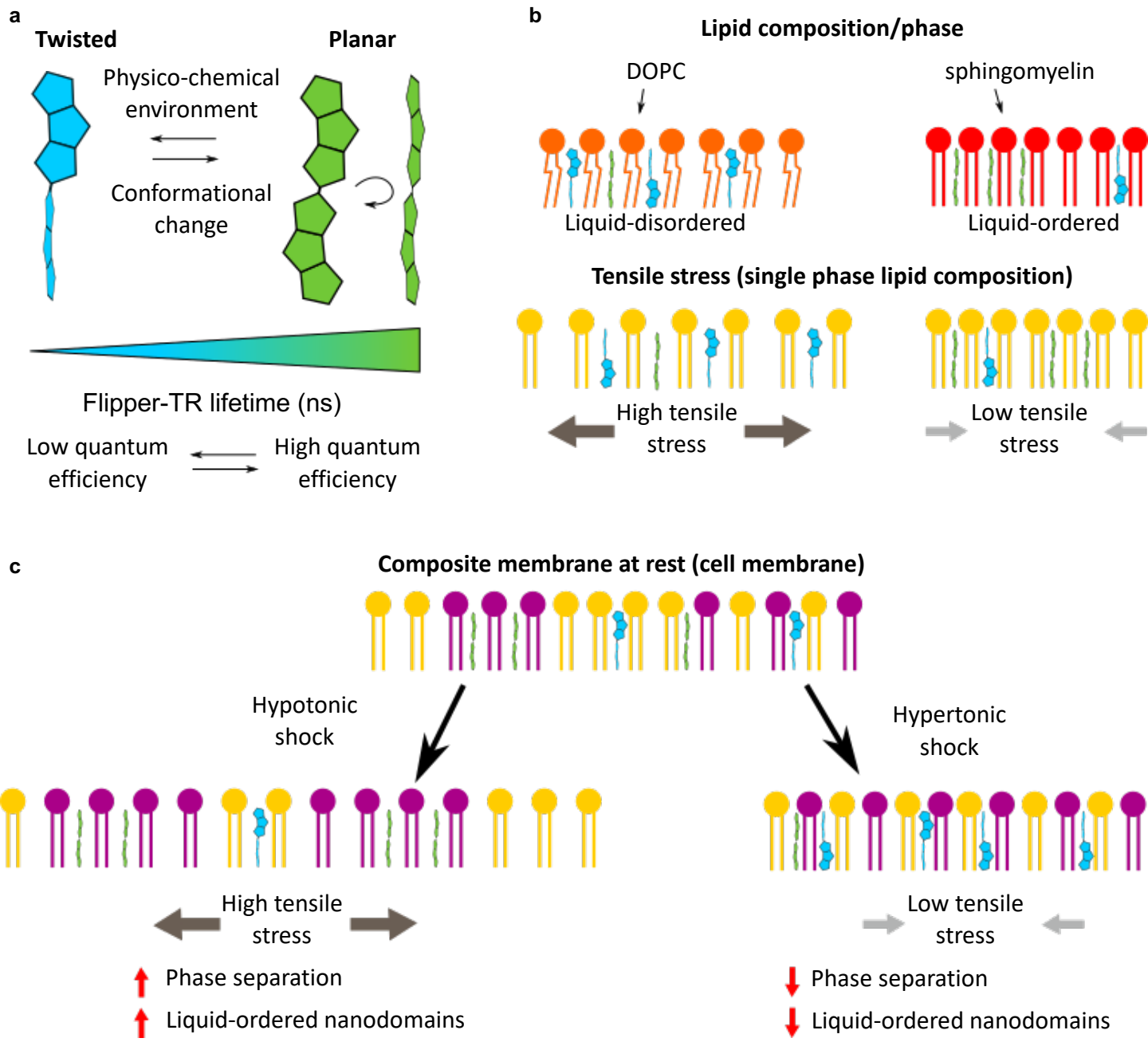

Figure 1: Principle of Flipper probe

(a) Flipper design is a planarizable push-pull system. Mechanical planarization is responsible for a spectrum of configurations from planar to twisted configuration, which will affect the photo-physics and notably the time of the excited state of the probe

(b) Lateral forces within the membrane directly set the twisting and therefore the photo-physics of the Flipper probes.

(c) In complex membrane (e.g cell membranes), high tensile stress will trigger phase separation and the formation of highly packed membrane nanodomains reported by an increase of Flippers lifetime

As the Flipper structure is mostly hydrophobic, the molecule spontaneously inserts in between hydrophobic tails of lipids that constitute cellular membranes (Fig 1b). When inserted, the hydrophobic forces that pack the lipids into a bilayer exert pressure onto the Flipper fluorophore and planarize it. Its planarization depends on the lipid composition, and in short, more ordered membranes exert more force and provide more planarization of Flippers and reversely, disordered membrane, less force and planarization.

The conformation (i.e. how much the Flipper molecule is planarized versus twisted) of the Flipper affects several parameters of the photophysics of the molecule: in the planarized state, the photon emission efficiency is increased by 10x compared to the most twisted state, and the peak of photon absorption is shifted towards larger wavelength, while the change is minimal for the emission peak [13].

-In particular, we noted that the lifetime of Flipper dramatically varied with lipid composition. The lifetime (Tau1 or the longest decay of a bi-exponential fit) in the twisted state, equivalent to highly disordered lipid membranes, was as small as 2.3 ns, while it could reach values as high as 7ns in highly ordered membranes, where the molecule is fully planarized. This large range of lifetime values is due to the fact that in the planarized state, fluorescence of the two fluorophores is coupled through an electron transfer from the donor group to the acceptor group[6], which delays emission of the photons, giving longer lifetimes.

-The range of lifetime values that this probe could cover was impressively large compared to other probes. For comparison, the lifetime of the Green Fluorescent Protein hardly varies around 2 ns[14]. We thus imagined that the Flippers are so sensitive that they could report tiny changes of the hydrophobic pressure linked to changes of membrane tension. Flipper is thus complementary to Laurdan, an organic fluorescent maker which allows by measuring its anisotropy to detect changes in plasma membrane fluidity. Since Flippers lifetime changes with both the lipid composition and membrane tension, changes of the lifetime can be directly associated with a change in membrane tension, only in cases where lipid composition is not changing. While this condition is always met in vitro, in cells, we usually consider that any variation of lifetime on the second timescale is related to membrane tension, as lipid composition hardly changes over this timescale. For longer timescales (minute, hour), appropriate controls that the lipid composition is not dramatically changing are required.

II-Staining biological samples with Flipper probes

Being hydrophobic, the probe is in the micellar form in aqueous solutions and is not fluorescent in this state. When the Flipper probe diffuses within lipid membranes, it inserts vertically between lipids and fluoresces. Thus, Flipper probes are "fluorogenic", becoming fluorescent only when inserted in the structure they target. We describe staining procedures, problems and solutions below.

A-Staining of cultured cells

To label most of the cell lines tested (Fig 2a), the probe, solubilized in DiMethylSulfOxide (DMSO), was normally directly added to the imaging medium at 1 uM final concentration and incubated 15 min at 37°C with cells. To keep a low concentration of DMSO in the final medium, 1 mM stock solutions of Flipper probes were usually made. In some cell types (MDCK, HeLa Kyoto and MZ), 5 min of Flipper incubation at 37°C might be enough to obtain good staining. However, at high cell density or in 3D cell cultures and tissues, longer incubation - in the order of a few hours - may be necessary. Imaging medium (Fluorobrite with Hepes or CO2 supply, or Leibovitz if no CO2 supply is available) was usually used and gave a good signal over noise ratio. The use of Foetal Bovine Serum (FBS) during staining and imaging can cause a lower signal, as it contains proteins which can extract hydrophobic molecules from membranes such as Albumin. However, we haven't observed a dramatic change of labelling efficiency using solutions described above supplemented with FBS. If the staining appears to be low with FBS, we nevertheless recommend testing solutions without it. We didn't observe drastic differences on the fluorescence intensity and lifetime of the probe between cells imaged at 37°C and the ones imaged at room temperature. Similarly, CO_2 adjunction in the imaging chamber or working with a medium supplemented with HEPES does not significantly impact Flipper fluorescence intensity or lifetime.

Importantly, the cell labelling occurs through a dynamic equilibrium of the probe with the micellar pool in the cell culture medium. Thus, a constant exchange of Flipper-TR between the plasma membrane and the medium occurs. This exchange is rapid for the Flipper-TR because the medium is directly in contact with the plasma membrane labelled by the probe. Using FRAP, we show a faster diffusion time at 37°C= 0.133 +/- 0.02 um2/sec (mobile fraction of 76% +/- 5) (Fig 2b, c) than at 20°C =0.09 um2/sec (Fig 2d). As expected, a decrease of plasma

FIGURE 2

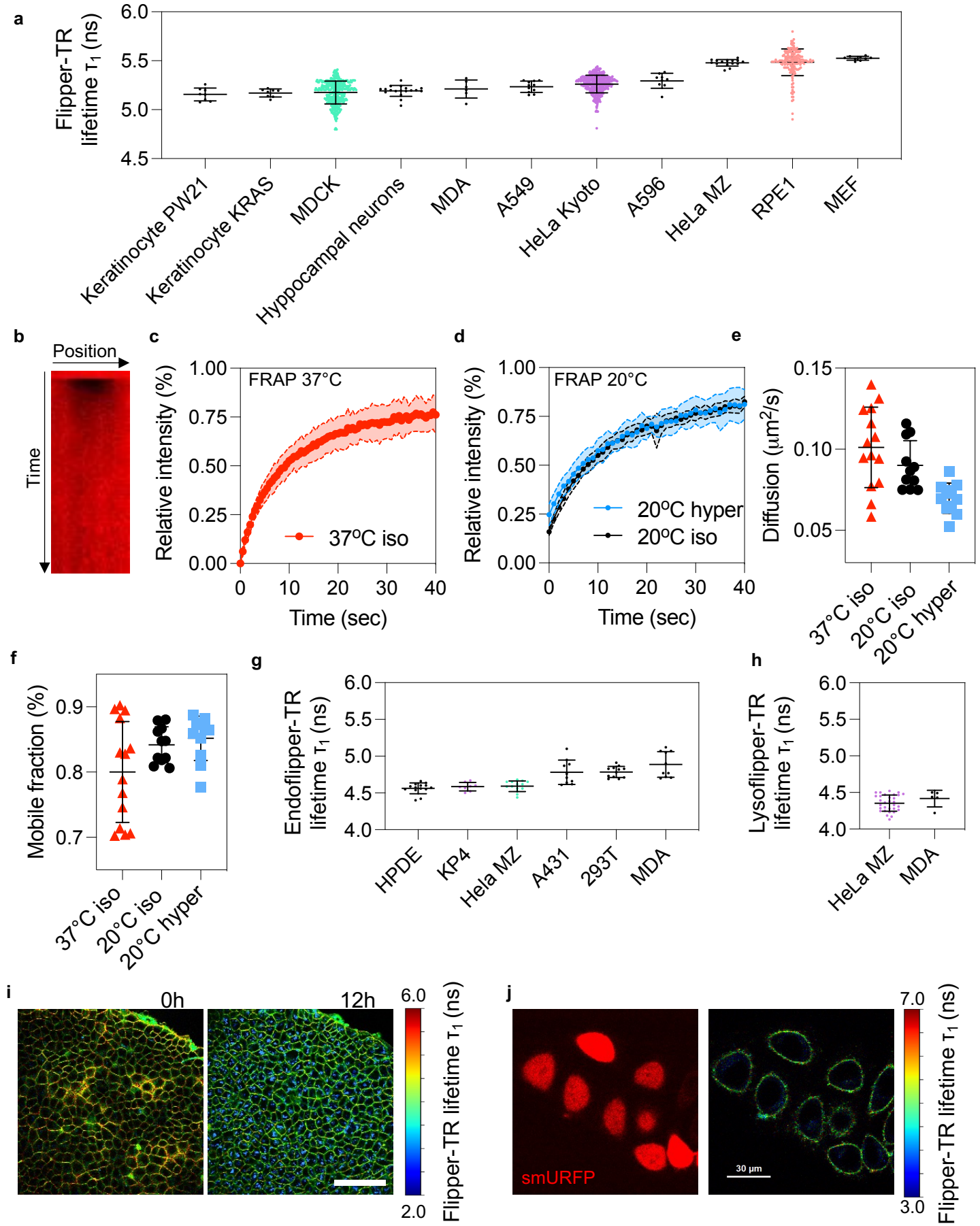
a
Flipper-TR lifetime τ1 (ns)
6.0
5.5
5.0
4.5
Keratinocyte PW21
Keratinocyte KRAS
MDCK
Hyppocampal neurons
MDA
A549
HeLa Kyoto
A596
HeLa MZ
RPE1
MEF
b
Position
Time
c
FRAP 37°C
Relative intensity (%)
1.00
0.75
0.50
0.25
0.00
37°C iso
0
10
20
30
40
Time (sec)
d
FRAP 20°C
Relative intensity (%)
20°C hyper
20°C iso
Time (sec)
e
Diffusion (μm²/s)
0.15
0.10
0.05
37°C iso
20°C iso
20°C hyper
f
Mobile fraction (%)
0.9
0.8
0.7
37°C iso
20°C iso
20°C hyper
g
Endoflipper-TR lifetime τ1 (ns)
6.0
5.5
5.0
4.5
4.0
HPDE
KP4
Hela MZ
A431
293T
MDA
h
Lysoflipper-TR lifetime τ1 (ns)
6.0
5.5
5.0
4.5
4.0
HeLa MZ
MDA
i
0h
12h
6.0
2.0
Flipper-TR lifetime τ1 (ns)
j
smURFP
30 μm
7.0
3.0
Flipper-TR lifetime τ1 (ns)

Figure 2: General behavior of Flipper probes

(a) Graph showing the Flipper-TR lifetime (τ1) extracted from different cell types

(b) Kymograph showing the recovery of Flipper-TR signal after bleaching at the plasma membrane (FRAP experiment)

(c) Graph showing FRAP curves of Flipper-TR at the plasma membrane at 37°C on HeLa cells in isotonic medium (n = 18)

(d) Graph showing FRAP curves of Flipper-TR at the plasma membrane at 22°C on HeLa cells in isotonic (320 mOsm) medium (n = 11) versus hypertonic (800 mOsm) medium (n = 10)

(e) Graph showing diffusion time coefficients (um^2/sec) extracted from graph (d) data

(f) Graph showing the mobile fractions (%) extracted from graph (d) data

(g) Graph showing the Lyso Flipper lifetime (τ1) extracted from different cell types (n>5 fields of view with at least 5 cells per field for each condition)

(h) Graph showing the Endo Flipper lifetime (τ1) extracted from different cell types (n>5 field of view with at least 5 cells per field for each condition)

(i) FLIM images showing MDCK tissue stained with Flipper-TR at different timepoints.

(j) Flipper-TR FLIM and confocal image of HeLa cells labelled with Flipper-TR lifetime and smURFP fluorescence

110 membrane tension induced by hypertonic treatment reduces the Flipper-TR diffusion time at
111 room temperature from 0.09 um2/sec to 0.07 um2/sec (Fig 2e) without impacting the mobile
112 fraction (Fig 2f).
113 We recommend, if possible, to keep a constant Flipper-TR concentration along the experiment.
114 Concerning Lyso Flipper-TR, the molecule diffuses freely across the plasma membrane and
115 quickly concentrates in the membrane of late endosomes and lysosomes (in a few minutes)
116 after headgroup protonation in this acidic environment. Consequently, for short timescale
117 experiments (less than 2h) it is not an issue to leave cells in Flipper medium containing Lyso
118 Flipper-TR. However, loss of the acidity of endosomal compartments after treatments or
119 change in the pH of the medium (due for example to phototoxicity) may trigger loss of the
120 Lyso Flipper-TR staining. The best labelling was obtained by incubating Lyso Flipper-TR at
121 1uM in Fluorobrite medium without serum for 20 minutes at 37°C prior to imaging.
122
123 Because of the dynamic exchange of the probe between the membrane and the medium,
124 washing Flipper labelled cells with medium containing FBS or BSA will decrease Flipper-TR
125 staining. Therefore, if washing is absolutely needed, it is recommended to wash with medium
126 without FBS, and/or keeping the concentration of the Flipper constant in the washes, which
127 will limit the decrease of the membrane signal.
128 The dynamic equilibrium is relatively long to reach (5-10 minutes), thus the photon count
129 depends on the time of incubation of cells with the probe, until it reaches a plateau value that
130 depends on your system. Incubations that are too long may lead to Flipper-TR endocytosis and
131 endosomal labelling. The Flipper-TR lifetimes within the endosomes are notably lower than in
132 the plasma membrane (Fig 2g, h), and we have never observed Flipper-TR labelling expanding
133 further away than from the endosomes (probably even the early endosomes). Also, the Flipper-
134 TR endosomal labelling appeared with various times depending on the cell types and
135 experimental conditions. In MDCK, we observed that endocytosis occurred after 12 hours (Fig
136 2i).
137 For long-term imaging experiments (several hours) with sufficient time-lapse between images,
138 we recommend performing sample-labelling for each time point: the sample is incubated with
139 Flipper-TR, imaged, and then the probe is washed away using medium with BSA or FBS. Each
140 timepoint requires re-incubation of the probe to prevent Flipper-TR endocytosis.
141

B-Co-staining with Flipper-TR

In order to specifically analyse the tension or lipid composition of a given organelle or during a biological process, it is possible to use other fluorescent probes or stable cell lines in conjunction with Flipper-TR. However, to avoid any fluorescence overlap with the probe, which could affect lifetime measurements, blue or far-red fluorescent dyes should be used (e.g: Organic dyes like Alexa-405 or Alexa-647 or Blue fluorescent protein, E2-Crimson or smURFP for fusion proteins, see Fig 2j). Indeed, due to the configuration of the probe (two heads), Flipper-TR has a large spectrum of emission and a large spectrum of absorption. The excitation peak of Flipper is at 485 nm and fluorescence emission is collected using a band pass 600/50 emission filter. Therefore, for example in the case of an organelle labelled with Alexa-405, excitation of this fluorophore (peak at 400 nm) will only weakly excite Flipper-TR, limiting the phototoxicity while the emission of Alexa-405 (400-530 nm) will not go through the FLIM detector and will not interfere with Flipper-TR lifetime measurement.

C-List of cells and organisms from which we obtained successful staining and imaging using Flipper probes

<u>List of cell types used with Flipper-TR</u>: HeLa MZ, HeLa Kyoto, MDCK, keratinocyte PW21, keratinocyte KRAS, hippocampal neurons, MDA, A549, A596, RPE1, MEF with lifetime value (tau1) ranging from 5 ns to 5.7 ns (Fig 2a).

<u>List of cell types used with Lyso-Flipper-TR</u>: HPDE, KP4, Hela MZ, A431, 293T, MDA with lifetime value (tau1) ranging from 4.4 ns to 5.1 ns (Fig 2g).

<u>List of cell types used with Endo Flipper-TR</u>: HeLa MZ, MDA with lifetime value (tau1) ranging from 4.1 ns to 4.7 ns (Fig 2h).

<u>List of organisms stained with Flipper-TR</u>: alginate capsules containing cells, PDMS tubes with attached cells on the inner surface, Arabidopsis thaliana leaf, Arabidopsis thaliana plant root, , Bacillus Subtilis (Fig 3i, j) or mouse embryos[15].

List of organisms where Flipper-TR staining does not work: E.Coli (gramm – cells)

FIGURE 3

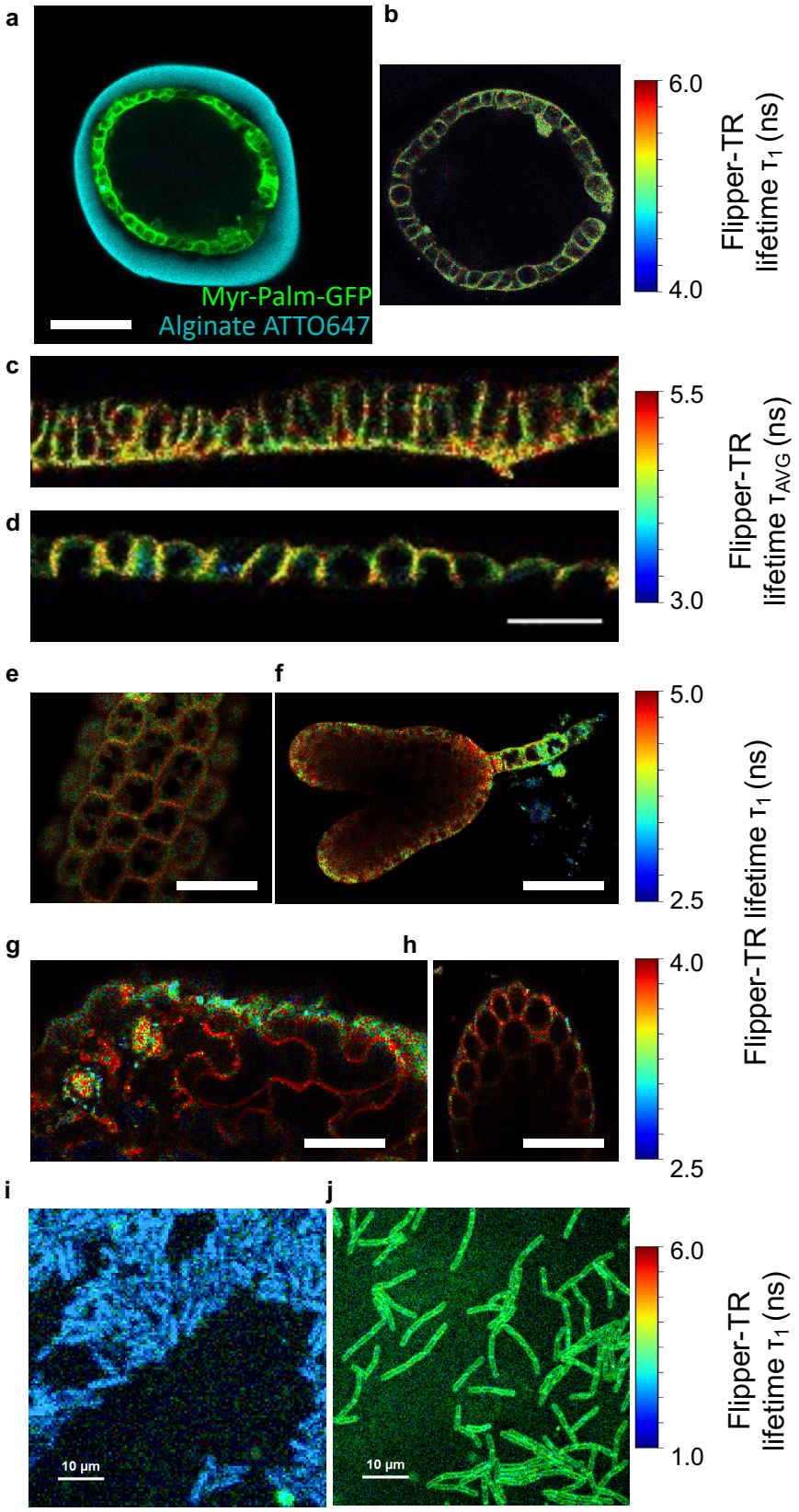
a
b
Myr-Palm-GFP
Alginate ATTO647
6.0
4.0
Flipper-TR lifetime τ1 (ns)
c
d
5.5
3.0
Flipper-TR lifetime τAVG (ns)
e
f
5.0
2.5
g
h
4.0
2.5
Flipper-TR lifetime τ1 (ns)
i
j
10 µm
10 µm
6.0
1.0
Flipper-TR lifetime τ1 (ns)

Figure 3: Flipper probes staining in various model and organisms

(a) Representative fluorescence image of a MDCK monolayer in an alginate capsule (Myr-Palm-GFP stain the MDCK cells and ATTO647 stain the alginate capsule in blue).

(b Representative FLIM image of an MDCK monolayer stained with Flipper-TR in an alginate capsule

(c) Representative FLIM bottom view of an MDCK monolayer stained with Flipper-TR in an alginate tube

(d) Representative FLIM side view of an MDCK monolayer stained with Flipper-TR in an alginate tube

(e) Representative FLIM image of Arabidopsis root stained with Flipper-TR

(f) Representative FLIM image of the entire Arabidopsis embryo stained with Flipper-TR

(g) Representative FLIM image of Arabidopsis leaf stained with Flipper-TR

(h) Representative FLIM image of Arabidopsis root stained with Flipper-TR

(i) Representative FLIM image of Gram-positive (B. subtilis) stained with Flipper-TR and

(j) Representative FLIM image of Gram-negative (E. coli) stained with Flipper-TR

D-Different probes for different staining

Various derivatives of Flipper were developed to target the endoplasmic reticulum (ER Flipper-TR), the mitochondria (Mito Flipper-TR),the lysosome/late endosome (Lyso Flipper-TR)[12] and more recently the early endosome (Endo Flipper-TR)[16] as well as a version of the probe for single-molecule super-resolution imaging of membrane tension (SR-Flipper[17,18]). The ER Flipper-TR selectively labels the membranes of endoplasmic reticulum via a pentafluorophenyl group which reacts with cysteine of proteins present on ER outer surface. The average lifetime of ER Flipper-TR is lower (3.5 ns in HeLa cells) than Flipper-TR (4.5 ns in HeLa cells) in various cell lines. The Mito Flipper-TR selectively labels the membranes of mitochondria via the interaction between the hydrophobic triphenylphosphonium cation with the negatively charged surface and the inside negative potential of the mitochondrial membrane. As observed for ER Flipper-TR, the average lifetime of Mito Flipper-TR is rather low (around 3.2 ns in HeLa cells).

Lyso Flipper-TR and Endo Flipper TR contain a morpholine headgroup of higher pKa in Endo Flipper-TR compared to Lyso Flipper-TR. This morpholine group is protonated in the acidic environment of endosomes and retained in its membrane. The average lifetime of Lyso Flipper-TR is around 4 ns in HeLa cells. Endo and Lyso Flipper-TR are showing very weak photo toxicity.

SR-Flipper is behaving as Flipper-TR (labelling plasma membrane in cells) and is reversibely switching from bright-state ketones to dark-state hydrates, hemiacetals, and hemithioacetals both in twisted and planarized state. It is therefore possible to use it for single-molecule localization microscopy and to resolve membranes well below the diffraction limit. The lifetime ($\tau 1$) of SR-Flipper is usually slightly lower (~10%) than the lifetime of Flipper-TR.HaloFlippers is based on the combination of the Flipper and a Halo tag to label any membrane of interest by targeting membrane specific protein labelled with a halo tag. Halo PhotoFlippers targets the nuclear membrane and the inner plasma membrane using a photocleavable domain[19].

III-Acquisition

Flipper probes have long average fluorescence lifetimes, up to 7 ns, which means that photons with lifetime up to 50 ns can be detected. Consequently, FLIM systems with sampling frequencies of 20 MHz have to be used in order to detect all the photons. On PicoQuant systems

208 the pulsed laser frequency can be set between 80 MHz and 31.25 kHz, but LEICA systems are
209 by default 80 MHz which will not allow to measure lifetimes higher than 12.5 ns. Therefore,
210 the sampling frequency has to be reduced in LEICA systems, using the pulse-picker device
211 (illuminates one out of 2 or more laser pulses), otherwise the lifetime will be underestimated.
212 Because of the the bi-exponential nature of the Flipper decay curve, it is important to record a
213 sufficient number of photons without saturating the detector. We recommend recording a
214 minimum intensity peak of 10^4 photons.
215
216 Another important point is that the phototoxicity during acquisition is lower when the laser
217 pulse frequency is decreased. With standard Time Correlated Single Photon Counting (TCSPC)
218 it is very important to have a count rate between 1 and 5% of the excitation rate (for 20MHz
219 pulse, average detector count rate shouldn't exceed 1 mHz) in order to maintain a low
220 probability of registering more than one photon per excitation cycle (with the dead time, the
221 system would detect the first photon and miss the second one, called "pile up" effect).
222 Other classic confocal microscopy parameters that participate in light acquisition (pinhole
223 aperture, laser power, pixel binning, scanning speed, size of the ROI, line averaging or
224 summation) may be used to optimize photon collection. Two technical innovation and process
225 also reduced the phototoxicity:
226 - Using a TCSPC device with reduced dead time (rapidFLIM from Picoquant, dead
227 time of less than 650 ps compare to 80 ns in normal FLIM) that allows to detect more than one
228 photon per excitation cycle. It also provides a better temporal resolution (see below) and allows
229 to work with higher intensities. Overall, with this new kind of TCSPC much higher detector
230 count rates can be processed while achieving better timing precision and faster acquisition.
231 - Repeating acquisition and summing-up photons from several images will allow to
232 obtain sufficient counts of photons (minimum peak of 10^4 events) for a correct fit. For standard
233 cells in culture, we used the following conditions. For example, using Flipper-TR in HeLa
234 Kyoto, we could sum up to 7 frames in a 256x256 pixel resolution to reach 10^5 photons peak
235 which was necessary for fitting procedure and lifetime extraction. Cell type and signal intensity
236 determine the optimal acquisition parameters. It is necessary to find a reasonable balance
237 between photon number and phototoxicity and we created a troubleshooting table based on our
238 experience (Fig 4).

FIGURE 4

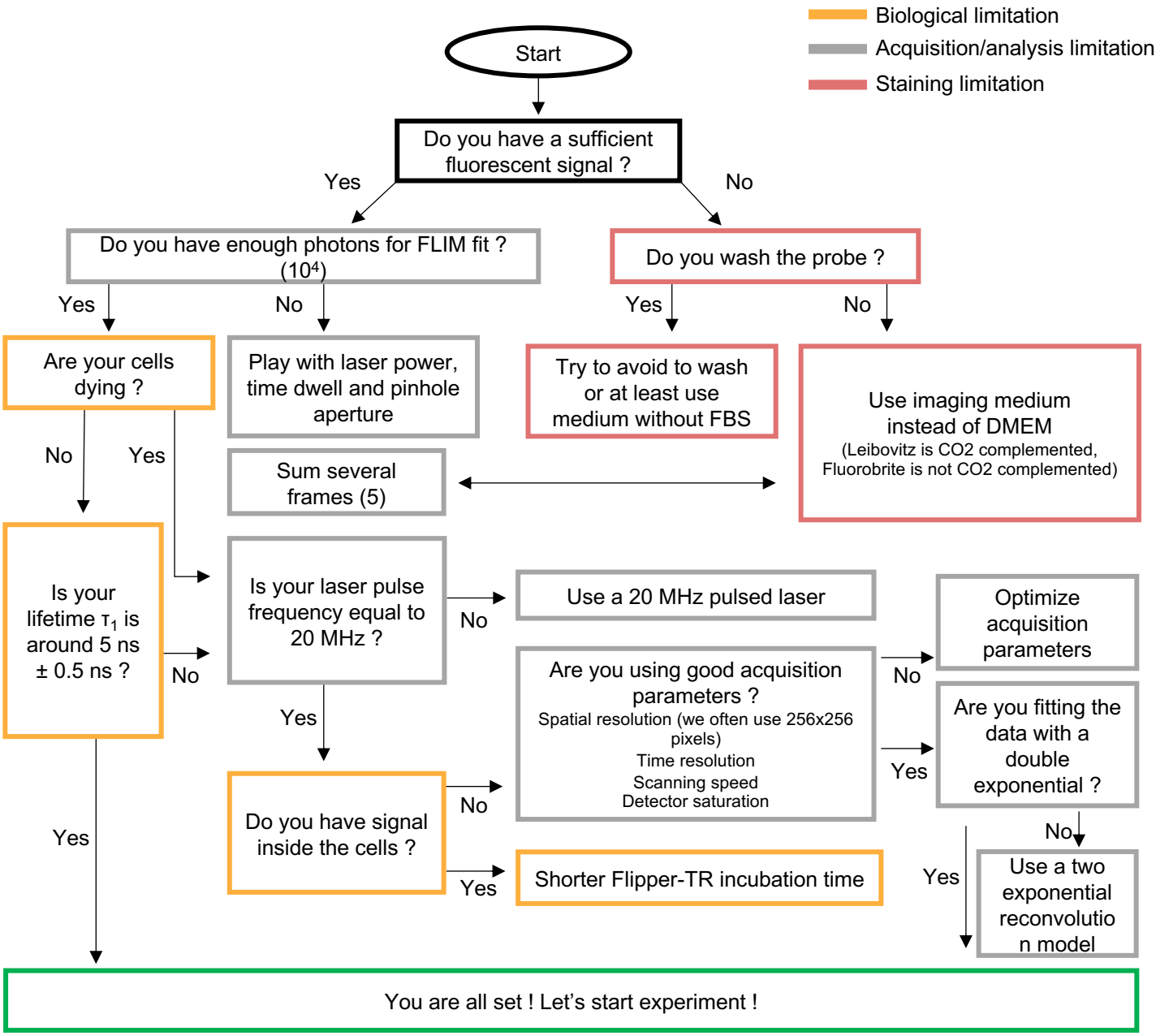

Figure 4: Chart to support users with troubleshooting Flipper probes experiments.

239

240 Timelapse of Flipper-TR

241 Since the Flipper-TR probe is in dynamic exchange with the environment, measuring lifetime
242 over time has its own loophole. If medium is added (osmotic shocks or drug addition), we
243 advise to keep Flipper-TR concentration constant. If medium is flowed (to test the effect of
244 shear stress for example) it is essential to keep the Flipper-TR concentration constant. Because
245 lifetime values are broad due to inherent biological variability and impacted by cell density or
246 cell type, we suggest assessing both lifetime variation and absolute lifetime values.

247

248 Combining Flipper probes with drug treatment

249 To measure the effect of a drug treatment on cells, we tested two strategies. (1) Imaging the
250 cells, adding the drug in the medium of a dish or replacing the medium with the one that
251 contains the drug using a microfluidic device and following the effect of the drug over time on
252 the same cells. This approach allows to eliminate the biological variability by measuring the
253 tension of the same cells before and after the treatment. (2) Imaging the control condition and
254 the treated condition independently (preferably acquire a large amount of cells to increase
255 statistics as it will be unpaired measurements, typically at least 15 fields of view per dish and
256 3 technical replicates). The treated cells must be imaged in the same conditions and on the same
257 day. Because steady state lifetime value can be variable (it depends on cell density), the control
258 condition must be repeated along every drug condition with the same seeding parameters. We
259 suggest following strategy (1) whenever possible. Classical solvents (DMSO) or antibiotics
260 used in inducible systems (doxycyclin) change the property of the membrane and therefore
261 affect the Flipper-TR lifetime. Indeed, DMSO increases solution hypertonicity while
262 doxycyclin affects cholesterol amounts.

263

264 Acquiring lifetime in a z-stack (such as in polarized tissue)

265 We observed a weak staining in very dense and polarized tissue independently of the incubation
266 time (from 5 min to 2h). Tissues are not perfectly flat leading to smaller collection of photons
267 at the apical side, which might lead to inhomogeneous signal and thus poorly reproducible
268 results. To compare lifetime of the Flipper-TR along Z-axis, samples and conditions, we
269 suggest defining the basal or mid-plane as the plane with the largest number of photons. Due
270 to the inherent difficulty to measure the lifetime of single cells, we advise to compare planes
271 containing several cells.

III-Analysis

A-Tools to analyse the data

Several companies have made commercial packages for FLIM analysis, but these are closed source tools that are not transparent in their analyses and typically only support their own file formats. Open source and user friendly tools have been and are being developed [20,21].

B-IRF (instrument response function)

In order to fit the signal, the contribution of instrumentation must be isolated. The overall timing precision of a complete TCSPC system is its Instrument Response Function (IRF). The best way to measure the IRF of the system is to use a fluorophore with similar fluorescence properties as the Flipper-TR but with a very short lifetime. The IRF can be measured using fluorescein solution quenched with potassium iodide before each experiment, or can be calculated (deducted) from the rising edge of the TCSPC histogram. The important point is to use the same IRF throughout the experiment. Software used to analyse FLIM images usually recalculate the IRF for each file by default.

C-Photon count fitting

Two different methods to fit the exponential decay exist: exponential reconvolution and exponential tailfit. A tailfit can be used when the lifetimes are significantly longer than the IRF. In general, a reconvolution fit is preferable, because the complete decay is fitted, while the start of the fitting range is slightly arbitrary for a tailfit. Depending on the format of the data and the available tools, choosing one or the other shouldn't impact measurements too much if enough photons are acquired. Tens of thousands of photons are required to accurately fit a bi-exponential decay [22]. In general, lifetime histograms of Flippers are not well fitted by a mono-exponential model, so it is standard to fit the data with double exponentials.

The exponential fitting can be done on a different set of pixels. The choice depends on the quality of your signal and the sensitivity of the effect you are looking at. (1) Whole photons analysis is the simplest and necessitate little requirement of input from the experimentalist, therefore increasing the reproducibility of the work. (2) It is possible in order to remove the

backround to apply a threshold on pixel intensity and only fit the corresponding pixels. It is however invalid to apply a threshold based on thelifetime values to extract lifetime. (2') Applying a threshold on the absolute lifetime value can be valid to create masks and separate objects with different Flipper lifetimes. For example, the lifetime of the plasma membrane is much higher than the lifetime of endosomal membrane, so a single FLIM image could be sufficient to discriminate the two objects. (3) Similar to (2), it is possible to overlap a mask generated from another channel to only select pixels of interest (Fig 5a-b).

Depending on the orientation of the cells in the beam, the number of photons can change. A side acquisition will give a lower number of photons than an acquisition from the bottom, leading to a worst fit (Fig 5c-e).

By fitting with a bi-exponential decay, two lifetimes will be extracted: τ_1 and τ_2. τ_{AVG} is an average between the 2 rates τ_1 and τ_2 weighted by the number of photons fitted by each parameter. τ_1 (the longest component) or τ_{AVG} will usually represent much higher photon counts than τ_2. Both τ_1 or τ_{AVG} will directly report the mechanical property of the probe so you should anyway take either τ_{AVG} or the longest τ (τ_1 on picoquant system) value to analyse tension fluctuations. In experiments analyzing the dynamics of Flipper, if the tendency of τ_1 and τ_{AVG} is different then it is probably due to a lack of photons for the fit and image acquisition must be optimized.

D- Image segmentation to extract Flipper lifetime

Here, we will develop two examples to illustrate the importance of extracting the lifetime properly. Fluorescence intensity images of a membrane probe (blue or far red CellMask for instance) can be used to generate a mask that permits to extract lifetime of all the pixels present in the mask (Fig 5a). Even if the lifetime of the internalized probe is lower than the lifetime of the probe at the plasma membrane, applying a threshold based on lifetime value will introduce a bias in the analysis of the overall lifetime. Considering only pixels corresponding to the plasma membrane instead of all the pixels of the image, which include signal coming from endosomes, gives a difference of 0.5 ns on average (Fig 5b).

The second example is illustrated by measuring the impact of blebbistatin (myosin inhibitor reducing cell contractility) on plasma membrane tension reported by Flipper-TR lifetime (Fig 5f). If all the pixels of the images (control versus blebbistatin-treated cells) are included for the fitting, a decrease of lifetime of 0.3 ns is observed (Fig 5g). However, it appears that on images

FIGURE 5

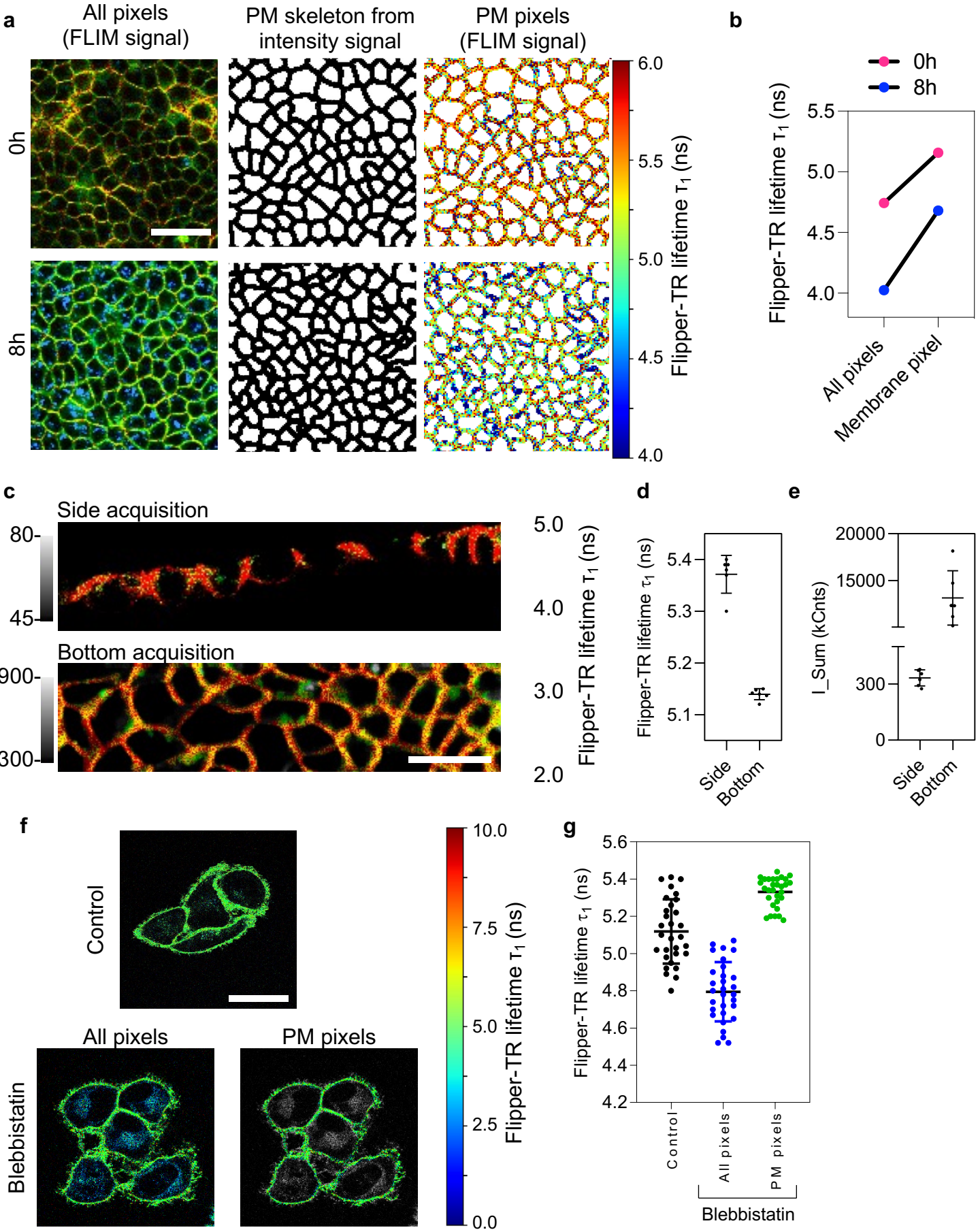
a
All pixels (FLIM signal)
PM skeleton from intensity signal
PM pixels (FLIM signal)
0h
8h
6.0
5.5
5.0
4.5
4.0
Flipper-TR lifetime τ1 (ns)
b
0h
8h
Flipper-TR lifetime τ1 (ns)
5.5
5.0
4.5
4.0
All pixels
Membrane pixel
c
Side acquisition
80
45
Bottom acquisition
900
300
5.0
4.0
3.0
2.0
Flipper-TR lifetime τ1 (ns)
d
Flipper-TR lifetime τ1 (ns)
5.4
5.3
5.2
5.1
Side
Bottom
e
I_Sum (kCnts)
20000
15000
300
0
Side
Bottom
f
Control
All pixels
PM pixels
Blebbistatin
10.0
7.5
5.0
2.5
0.0
Flipper-TR lifetime τ1 (ns)
g
Flipper-TR lifetime τ1 (ns)
5.6
5.4
5.2
5.0
4.8
4.6
4.4
4.2
Control
All pixels
PM pixels
Blebbistatin

Figure 5: How to properly extract the Flipper-TR lifetime from FLIM image.

(a) Representative FLIM images of MDCK tissue stained with Flipper-TR (top row) with and without endosomal staining (respectively top panel and bottom panel after 8h of incubation) due to longer cell incubation with Flipper-TR. Flipper-TR lifetime of pixels corresponding only to plasma membrane (PM) extracted via the segmentation of the PM (middle column) based on Flipper-TR fluorescence intensity

(b) Graph showing the Flipper-TR lifetime (τ1, ns) extracted from all the pixels of the image versus only the pixels corresponding to the plasma membrane.

(c) Representative FLIM images of MDCK tissue stained with Flipper-TR acquired from the side (top row) or from the bottom (bottom row).

(d) Graph showing the Flipper-TR lifetime (τ1, ns) extracted from the pixels of the side acquisition image versus from the bottom acquisition image.

(e) Graph showing the number of photons extracted from the pixels of the side acquisition image versus from the bottom acquisition image.

(f) Representative FLIM images of HeLa cells incubated with DMSO (top) or with blebbistatin (bottom). Bottom images show two configurations: all the pixels are selected (left) or only pixels corresponding to PM were manually selected (right).

(g) Graph showing Flipper-TR lifetime quantification corresponding to (c). Lifetime (τ1, ns) was extracted from all the pixels of the image versus only the pixels corresponding to the plasma membrane (n=30 for both control and blebbistatin treated cells)

of Blebbistatin-treated cells, despite an identical Flipper-TR incubation time, many intracellular membranes with a low lifetime around 2.5 ns are visible. These pixels likely contribute to the overall lower lifetime measured for Blebbistatin-treated cells. By contrast, if only plasma membrane lifetime is measured, the average lifetime of Blebbistatin-treated cells is 0.1 ns higher than the average lifetime of control cells. Directly selecting the plasma membrane pixels also excludes the background, which could affect the analysis.

E-Comparing different areas within the same image

The goal of the experiments might be to compare regions within the same image. As explained, a minimum number of photons will be necessary to obtain a decent fit and to extract the lifetime properly. Therefore, we strongly suggest to check that the photon count is similar between different analyzed area.

IV-Results

A-Different lifetime along cell height

By imaging Flipper-TR over z-stacks of MDCK polarized tissues, we observed a lower lifetime (4.6 ns) at the basal plane of the cell compared to the apical plane (5.4 ns), as illustrated in Fig 6a. Also, large variability exists between position in the dish: the basal plane lifetime values vary from 4.2 ns to 5.1 ns, while the apical plane values vary between 4.3 ns and 5.6 ns. However, the lifetime difference between basal and apical planes is always the same (Fig 6b) which could be explained by different lipid compositions. Therefore, single plane imaging of cells to compare, for example, different treatments, must be performed at a similar height (Fig 6c), and sufficient statistics to account for large biological differences between single cells are required.

B-Mitotic cells have a more disordered plasma membrane

We analyzed the Flipper-TR lifetime in mitotic cells which are known to have a higher volume, higher cortical tension and a very different shape than adherent cells[23–25]. Mitotic cells were identified by eye based on their rounded shape and their limited attached surface to the glass bottom. In contrast to the literature, mitotic cells have a 0.35 ns lower lifetime (Fig 6d)

FIGURE 6

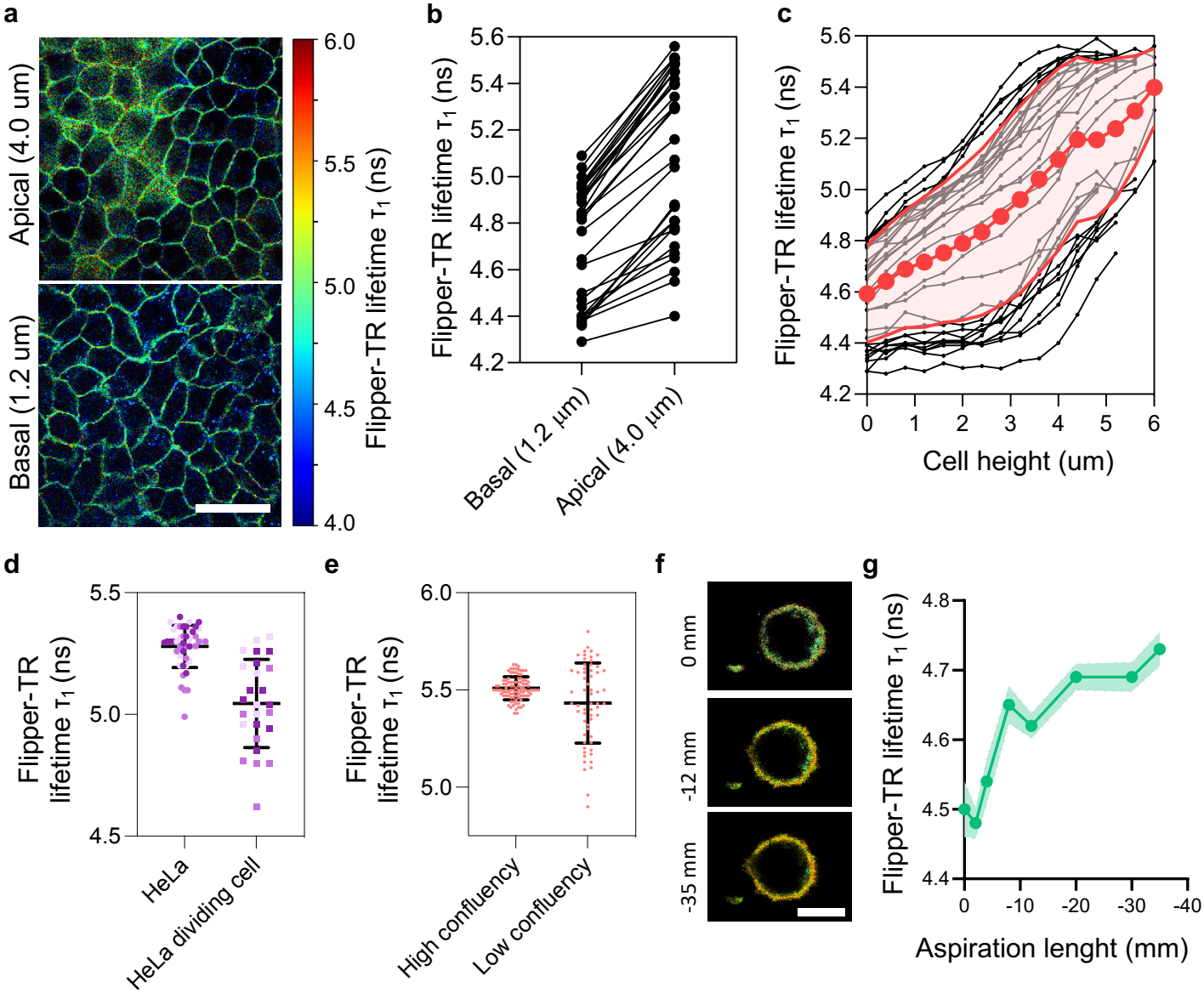
a
Apical (4.0 um)
Basal (1.2 um)
6.0
5.5
5.0
4.5
4.0
Flipper-TR lifetime τ1 (ns)
b
Flipper-TR lifetime τ1 (ns)
5.6
5.4
5.2
5.0
4.8
4.6
4.4
4.2
Basal (1.2 µm)
Apical (4.0 µm)
c
Flipper-TR lifetime τ1 (ns)
5.6
5.4
5.2
5.0
4.8
4.6
4.4
4.2
0
1
2
3
4
5
6
Cell height (um)
d
Flipper-TR lifetime τ1 (ns)
5.5
5.0
4.5
HeLa
HeLa dividing cell
e
Flipper-TR lifetime τ1 (ns)
6.0
5.5
5.0
High confluency
Low confluency
f
0 mm
-12 mm
-35 mm
g
Flipper-TR lifetime τ1 (ns)
4.8
4.7
4.6
4.5
4.4
0
-10
-20
-30
-40
Aspiration lenght (mm)

Figure 6: Flipper-TR lifetime is affected by several parameters

(a) Representative FLIM images of MDCK tissue stained with Flipper-TR in the apical plan (top row) ant the basal plan (bottom row)

(b) Graph showing the quantification of Flipper-TR lifetime (ns) in the apical plane (4.0 micron from the bottom) and the basal plane (1.2 micron from the bottom). The bottom was determined as the plane with the highest number of photons (n = 45).

(c) Graph showing the quantification of Flipper-TR lifetime (τ1, ns) from the bottom plane to the apical plane by steps of 0.4 micron. Each curve represents the lifetime of an entire field of view (n = 45).

(d) Graph showing the quantification of Flipper-TR lifetime (τ1, ns) in mitotic and non-mitotic HeLa cells

(e) Graph showing the quantification of Flipper-TR lifetime (τ1, ns) in confluent and non-confluent RPE1 cells

(f) Representative Flipper-TR FLIM images of HeLa cell aspirated in a micropipette at different aspiration pressure. Scale bar: 10 µm

(g) Graph showing the quantification corresponding to (c) of Flipper-TR lifetime (τ1, ns) depending on the aspiration pressure applied to the cell.

373 compared to adherent cells[24,25], while one might have expected an increase of Flipper-TR
374 lifetime. This lower lifetime could reflect a change of lipid composition during cell division,
375 itself causing increased membrane fluidity in mitotic cells[26].
376

377 C- Flipper-TR variability depends on cell confluency

378
379 We analyzed the Flipper-TR lifetime depending on cell confluency. Using RPE1, we observed
380 that confluent cells have a Flipper-TR lifetime centered around 5.5 +/- 0.06 ns while non-
381 confluent cell lifetime is centered around 5.4 +/- 0.23 ns (Fig. 6e). Therefore, in case of
382 experiments performed using cells at low confluency, sufficient statistics are required to
383 account for large biological differences between single cells.
384

385 D- Distinguishing the contributions of lipid composition and tension to the
386 changes of lifetime

387
388 Previous work from the lab[8] showed that mechanical increase of Giant Unilamellar Vesicles
389 (GUVs) membrane tension induced by micropipette aspiration (high tension) leads to an
390 increase of 0.2 ns of Flipper-TR lifetime. Using the same setup to aspirate HeLa cells in
391 suspension (Fig 6f, an increase of 0.2 ns was also observed (Fig 6g), confirming that in both
392 GUVs and cells Flipper-TR lifetime measurements can directly report a mechanically induced
393 change of membrane tension.
394 Although being slightly lower than Flipper (steady state lifetime of 5 ns vs 5.8 ns for SM/Chol
395 GUV), the lifetime of super-resolution (SR)-Flipper also reports changes in membrane tension
396 of GUVs (Fig 7a-b) as well as change in lipid packing (composition). Indeed, SR-Flipper-TR
397 lifetime of SM/Chol (70/30) GUV is centred around 5 ns while the lifetime of DOPC/Chol
398 (70/30) GUV is centred around 4.2 ns (Fig 7b). With both lipid compositions, SR-Flipper
399 lifetime decreases upon membrane tension decrease induced by hypertonic shocks proving that
400 Flipper probes lifetime report both lipid composition and membrane tension (Fig 7a-e). In
401 contrast, the lifetime of pure DOPC GUVs is not changing after hypertonic shock which is in
402 good agreement with an absence of phase separation (Fig 7a,f).
403 NNiemann-Pick C1 protein (NPC1) is responsible of the intracellular transport of Cholesterol
404 and shingolipids. Consequently, the depletion of NPC1 is responsible for cholesterol
405 accumulation in endosomes. Consistently, LysoFlipper in HeLa MZ NPC1 KO cells have a
406 higher lifetime than in WT HeLa cells indicating higher lipid packing (Fig 7g-h). Nonetheless,

FIGURE 7

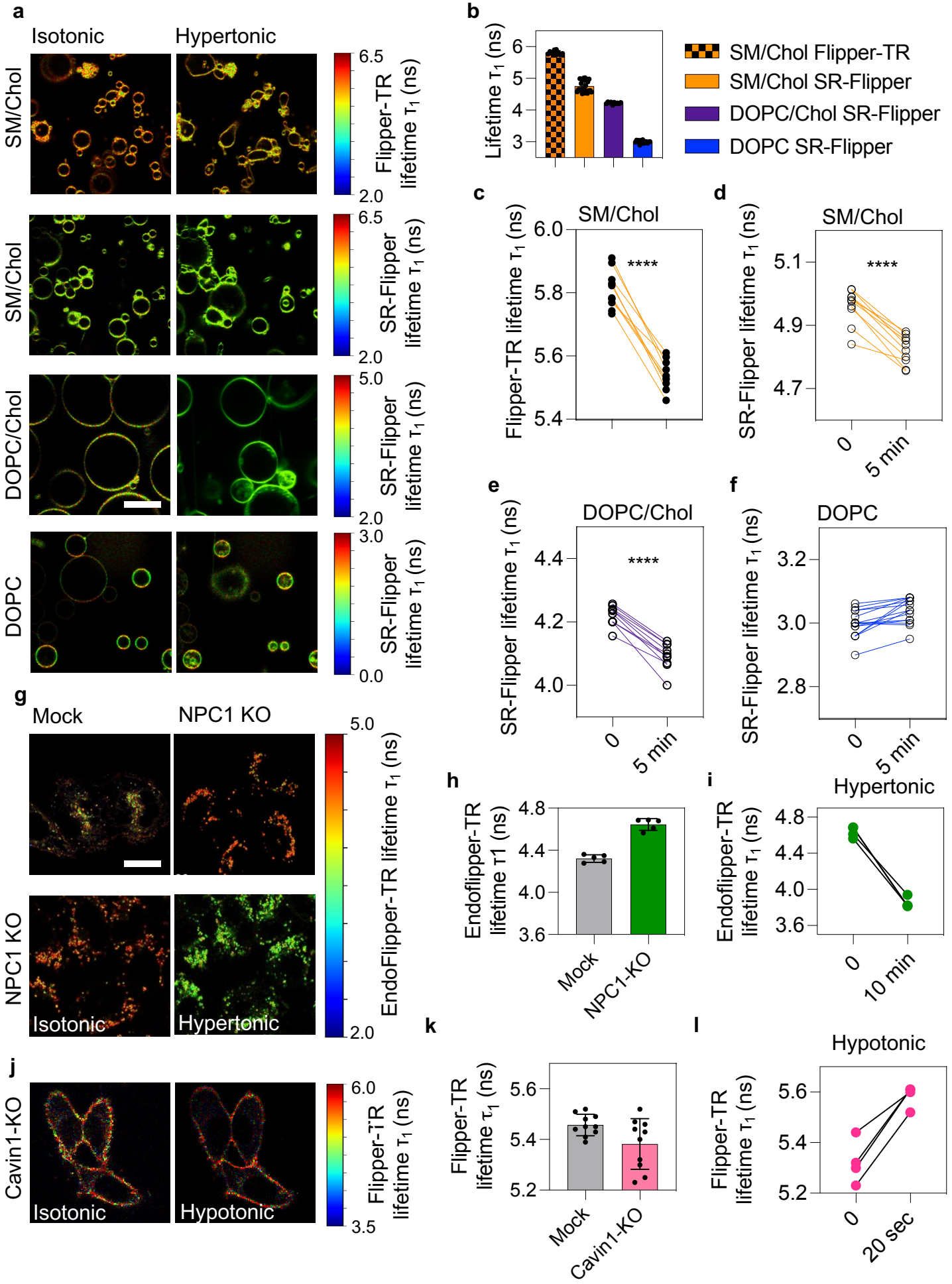
a
Isotonic
Hypertonic
SM/Chol
SM/Chol
DOPC/Chol
DOPC
Flipper-TR lifetime τ1 (ns)
SR-Flipper lifetime τ1 (ns)
6.5
2.0
5.0
3.0
0.0
b
Lifetime τ1 (ns)
SM/Chol Flipper-TR
SM/Chol SR-Flipper
DOPC/Chol SR-Flipper
DOPC SR-Flipper
c
SM/Chol
Flipper-TR lifetime τ1 (ns)
****
d
SM/Chol
SR-Flipper lifetime τ1 (ns)
0
5 min
e
DOPC/Chol
f
DOPC
g
Mock
NPC1 KO
Isotonic
Hypertonic
EndoFlipper-TR lifetime τ1 (ns)
h
Endoflipper-TR lifetime τ1 (ns)
Mock
NPC1-KO
i
Hypertonic
10 min
j
Cavin1-KO
Hypotonic
k
l
20 sec

Figure 7: Flipper lifetime allow to detect membrane tension variations although if lipid composition is different.

(a) Representative FLIM images before and after hypertonic shocks of SM/Chol containing GUVs stained with Flipper-TR or SR-Flipper, DOPC/Chol containing GUVs stained with SR-Flipper and of DOPC containing GUVs stained with SR-Flipper (d).

(b) Graph showing the quantification of Flipper-TR and SR-Flipper lifetime (τ1, ns) before hypertonic shock on GUV of specified lipid composition.

(c) Graph showing the quantification of Flipper-TR lifetime (τ1, ns) before and after hypertonic shock on SM/Chol GUV.

(d-f) Graph showing the quantification of SR-Flipper lifetime (τ1, ns) before and after hypertonic shock on GUV of specified lipid composition.

(g) Top : representative Endo Flipper FLIM images of HeLa MZ cells (left) and HeLa MZ NPC1 KO cells (right), which present accumulation of Cholesterol in endosomes. Bottom : representative Endo Flipper FLIM images of HeLa MZ NPC1 KO cells before hypertonic shock (left) and after hypertonic shock (right).

(h) Graph showing the quantification of Endo Flipper lifetime (ns) of HeLa MZ cells and HeLa MZ NPC1 KO cells

(i) Graph showing the quantification of Endo Flipper lifetime (τ1, ns) before and after hypertonic shock

(j) Representative Flipper-TR FLIM images of HeLa Cavin1-KO cells before hypotonic shock (left) and after hypotonic shock (right).

(j) Graph showing the quantification of Flipper-TR lifetime (τ1, ns) in HeLa cells (n = 10) and HeLa Cavin1-KO cells (n = 10) in isotonic medium.

(k) Graph showing the quantification of Flipper-TR lifetime (τ1, ns) in HeLa Cavin1-KO cells (n = 4) after a hypotonic shock

---

i

407 the probe is still able to report a change in membrane tension, as demonstrated by lifetime
408 decrease under hypertonic treatment (Fig 7g,i).
409 The protein Cavin1 is a major component of caveolae and its deletion prevents caveolae
410 assembly[10,27]. Interestingly, this absence of caveolae is associated with a smaller Flipper-TR
411 lifetime, indicating either a lower membrane tension or a more disordered membrane
412 composition (Fig 7j-k). Cavin1-KO cells show a lifetime increase upon hypotonic shocks (Fig
413 7j,i). Despite a potential difference of lipid composition, Flipper-TR is anyway able to report
414 an increase of membrane tension.
415

416 Conclusion:

417 Here, we have reported the current technical difficulties we faced using Flipper probes, and
418 how we overcame them. In the future, further developments of Flipper probes will allow us to
419 bypass some of these problems. Technical improvements in the FLIM image acquisition and
420 analysis may also help spread the use of Flipper probes to all biological samples of interest.
421 Flipper probes remain an interesting tool for many applications, and in some cases, the only
422 available tool to measure membrane tension.

Bibliography

(1) Roca-Cusachs, P.; Conte, V.; Trepat, X. Quantifying Forces in Cell Biology. *Nat. Cell Biol.* **2017**, *19* (7), 742–751. https://doi.org/10.1038/ncb3564.

(2) Abella, M.; Andruck, L.; Malengo, G.; Skruzny, M. Actin-Generated Force Applied during Endocytosis Measured by Sla2-Based FRET Tension Sensors. *Dev. Cell* **2021**, *56* (17), 2419-2426.e4. https://doi.org/10.1016/j.devcel.2021.08.007.

(3) Déjardin, T.; Carollo, P. S.; Sipieter, F.; Davidson, P. M.; Seiler, C.; Cuvelier, D.; Cadot, B.; Sykes, C.; Gomes, E. R.; Borghi, N. Nesprins Are Mechanotransducers That Discriminate Epithelial-Mesenchymal Transition Programs. *J. Cell Biol.* **2020**, *219* (10), e201908036. https://doi.org/10.1083/jcb.201908036.

(4) Li, W.; Yu, X.; Xie, F.; Zhang, B.; Shao, S.; Geng, C.; Aziz, A. ur R.; Liao, X.; Liu, B. A Membrane-Bound Biosensor Visualizes Shear Stress-Induced Inhomogeneous Alteration of Cell Membrane Tension. *iScience* **2018**, *7*, 180–190. https://doi.org/10.1016/j.isci.2018.09.002.

(5) Páez-Pérez, M.; López-Duarte, I.; Vyšniauskas, A.; Brooks, N. J.; Kuimova, M. K. Imaging Non-Classical Mechanical Responses of Lipid Membranes Using Molecular Rotors. *Chem Sci* **2021**, *12* (7), 2604–2613. https://doi.org/10.1039/D0SC05874B.

(6) Assies, L.; García-Calvo, J.; Piazzolla, F.; Sanchez, S.; Kato, T.; Reymond, L.; Goujon, A.; Colom, A.; López-Andarias, J.; Straková, K.; Mahecic, D.; Mercier, V.; Riggi, M.; Jiménez-Rojo, N.; Roffay, C.; Licari, G.; Tsemperouli, M.; Neuhaus, F.; Fürstenberg, A.; Vauthey, E.; Hoogendoorn, S.; Gonzalez-Gaitan, M.; Zumbuehl, A.; Sugihara, K.; Gruenberg, J.; Riezman, H.; Loewith, R.; Manley, S.; Roux, A.; Winssinger, N.; Sakai, N.; Pitsch, S.; Matile, S. Flipper Probes for the Community. *Chim. Int. J. Chem.* **2021**, *75* (12), 1004–1011. https://doi.org/10.2533/chimia.2021.1004.

(7) Soleimanpour, S.; Colom, A.; Derivery, E.; Gonzalez-Gaitan, M.; Roux, A.; Sakai, N.; Matile, S. Headgroup Engineering in Mechanosensitive Membrane Probes. *Chem. Commun.* **2016**, *52* (100), 14450–14453. https://doi.org/10.1039/C6CC08771J.

(8) Colom, A.; Derivery, E.; Soleimanpour, S.; Tomba, C.; Molin, M. D.; Sakai, N.; González-Gaitán, M.; Matile, S.; Roux, A. A Fluorescent Membrane Tension Probe. *Nat. Chem.* **2018**, *10* (11), 1118–1125. https://doi.org/10.1038/s41557-018-0127-3.

(9) Mercier, V.; Larios, J.; Molinard, G.; Goujon, A.; Matile, S.; Gruenberg, J.; Roux, A. Endosomal Membrane Tension Regulates ESCRT-III-Dependent Intra-Lumenal Vesicle Formation. *Nat. Cell Biol.* **2020**, *22* (8), 947–959. https://doi.org/10.1038/s41556-020-0546-4.

(10) Roffay, C.; Molinard, G.; Kim, K.; Urbanska, M.; Andrade, V.; Barbarasa, V.; Nowak, P.; Mercier, V.; García-Calvo, J.; Matile, S.; Loewith, R.; Echard, A.; Guck, J.; Lenz, M.; Roux, A. Passive Coupling of Membrane Tension and Cell Volume during Active Response of Cells to Osmosis. *Proc. Natl. Acad. Sci.* **2021**, *118* (47). https://doi.org/10.1073/pnas.2103228118.

(11) Lachuer, H.; Le, L.; Lévêque-Fort, S.; Goud, B.; Schauer, K. Membrane Tension Spatially Organizes Lysosomal Exocytosis. bioRxiv April 22, 2022, p 2022.04.22.489160. https://doi.org/10.1101/2022.04.22.489160.

(12) Goujon, A.; Colom, A.; Straková, K.; Mercier, V.; Mahecic, D.; Manley, S.; Sakai, N.; Roux, A.; Matile, S. Mechanosensitive Fluorescent Probes to Image Membrane Tension in Mitochondria, Endoplasmic Reticulum, and Lysosomes. *J. Am. Chem. Soc.* **2019**, *141* (8), 3380–3384. https://doi.org/10.1021/jacs.8b13189.

(13) Dal Molin, M.; Verolet, Q.; Colom, A.; Letrun, R.; Derivery, E.; Gonzalez-Gaitan, M.; Vauthey, E.; Roux, A.; Sakai, N.; Matile, S. Fluorescent Flippers for Mechanosensitive Membrane Probes. *J. Am. Chem. Soc.* **2015**, *137* (2), 568–571. https://doi.org/10.1021/ja5107018.

(14) Davidson, N. M.; Gallimore, P. J.; Bateman, B.; Ward, A. D.; Botchway, S. W.; Kalberer, M.; Kuimova, M. K.; Pope, F. D. Measurement of the Fluorescence Lifetime of GFP in High Refractive Index Levitated Droplets Using FLIM. *Phys. Chem. Chem. Phys.* **2020**, *22* (26), 14704–14711. https://doi.org/10.1039/C9CP06395A.

(15) Royer, C.; Sandham, E.; Slee, E.; Schneider, F.; Lagerholm, C. B.; Godwin, J.; Veits, N.; Hathrell, H.; Zhou, F.; Leonavicius, K.; Garratt, J.; Narendra, T.; Vincent, A.; Jones, C.; Child, T.; Coward, K.; Graham, C.; Fritzsche, M.; Lu, X.; Srinivas, S. ASPP2 Maintains the Integrity of Mechanically Stressed Pseudostratified Epithelia during Morphogenesis. *Nat. Commun.* **2022**, *13* (1), 941. https://doi.org/10.1038/s41467-022-28590-4.

(16) Piazzolla, F.; Mercier, V.; Assies, L.; Sakai, N.; Roux, A.; Matile, S. Fluorescent Membrane Tension Probes for Early Endosomes. *Angew. Chem.* **2021**, *133* (22), 12366–12371. https://doi.org/10.1002/ange.202016105.

(17) García-Calvo, J.; López-Andarias, J.; Maillard, J.; Mercier, V.; Roffay, C.; Roux, A.; Fürstenberg, A.; Sakai, N.; Matile, S. HydroFlipper Membrane Tension Probes: Imaging Membrane Hydration and Mechanical Compression Simultaneously in Living Cells. *Chem. Sci.* **2022**, *13* (7), 2086–2093. https://doi.org/10.1039/d1sc05208j.

(18) García-Calvo, J.; Maillard, J.; Fureraj, I.; Strakova, K.; Colom, A.; Mercier, V.; Roux, A.; Vauthey, E.; Sakai, N.; Fürstenberg, A.; Matile, S. Fluorescent Membrane Tension Probes for Super-Resolution Microscopy: Combining Mechanosensitive Cascade Switching with Dynamic-Covalent Ketone Chemistry. *J. Am. Chem. Soc.* **2020**, *142* (28), 12034–12038. https://doi.org/10.1021/jacs.0c04942.

(19) López-Andarias, J.; Eblighatian, K.; Pasquer, Q. T. L.; Assies, L.; Sakai, N.; Hoogendoorn, S.; Matile, S. Photocleavable Fluorescent Membrane Tension Probes: Fast Release with Spatiotemporal Control in Inner Leaflets of Plasma Membrane, Nuclear Envelope, and Secretory Pathway. *Angew. Chem. Int. Ed.* **2022**, *61* (1), e202113163. https://doi.org/10.1002/anie.202113163.

(20) Gao, D.; Barber, P. R.; Chacko, J. V.; Sagar, M. A. K.; Rueden, C. T.; Grislis, A. R.; Hiner, M. C.; Eliceiri, K. W. FLIMJ: An Open-Source ImageJ Toolkit for Fluorescence Lifetime Image Data Analysis. *PLOS ONE* **2020**, *15* (12), e0238327.

https://doi.org/10.1371/journal.pone.0238327.

(21) Warren, S. C.; Margineanu, A.; Alibhai, D.; Kelly, D. J.; Talbot, C.; Alexandrov, Y.; Munro, I.; Katan, M.; Dunsby, C.; French, P. M. W. Rapid Global Fitting of Large Fluorescence Lifetime Imaging Microscopy Datasets. *PLOS ONE* **2013**, *8* (8), e70687. https://doi.org/10.1371/journal.pone.0070687.

(22) Köllner, M.; Wolfrum, J. How Many Photons Are Necessary for Fluorescence-Lifetime Measurements? *Chem. Phys. Lett.* **1992**, *200* (1), 199–204. https://doi.org/10.1016/0009-2614(92)87068-Z.

(23) Zlotek-Zlotkiewicz, E.; Monnier, S.; Cappello, G.; Le Berre, M.; Piel, M. Optical Volume and Mass Measurements Show That Mammalian Cells Swell during Mitosis. *J. Cell Biol.* **2015**, *211* (4), 765–774. https://doi.org/10.1083/jcb.201505056.

(24) Fischer-Friedrich, E.; Hyman, A. A.; Jülicher, F.; Müller, D. J.; Helenius, J. Quantification of Surface Tension and Internal Pressure Generated by Single Mitotic Cells. *Sci. Rep.* **2014**, *4* (1), 1–8. https://doi.org/10.1038/srep06213.

(25) Stewart, M. P.; Helenius, J.; Toyoda, Y.; Ramanathan, S. P.; Muller, D. J.; Hyman, A. A. Hydrostatic Pressure and the Actomyosin Cortex Drive Mitotic Cell Rounding. *Nature* **2011**, *469* (7329), 226–230. https://doi.org/10.1038/nature09642.

(26) Atilla-Gokcumen, G. E.; Muro, E.; Relat-Goberna, J.; Sasse, S.; Bedigian, A.; Coughlin, M. L.; Garcia-Manyes, S.; Eggert, U. S. Dividing Cells Regulate Their Lipid Composition and Localization. *Cell* **2014**, *156* (3), 428–439. https://doi.org/10.1016/j.cell.2013.12.015.

(27) Andrade, V.; Bai, J.; Gupta-Rossi, N.; Jimenez, A. J.; Delevoye, C.; Lamaze, C.; Echard, A. Caveolae Promote Successful Abscission by Controlling Intercellular Bridge Tension during Cytokinesis. *Sci. Adv. 8* (15), eabm5095. https://doi.org/10.1126/sciadv.abm5095.